*Progress In Electromagnetics Research B, Vol. 10, 105–116, 2008*

# VELOCITY ERROR ANALYSIS OF A K-BAND DUAL MODE TRAFFIC RADAR

**M.-H. Yang, J. Xu, and X.-W. Sun** †

Shanghai Institute of Microsystems
and Information Technology of CAS
Shanghai 200050, China

**Abstract**—This paper is addressed to a design of K-band dual mode radar used in traffic information collection. The radar can work in both Frequency Modulate Continual Wave (FMCW) mode and Continual Wave (CW) mode. As VCO is seldom used as the oscillator in CW radar for velocity measurement, this paper studied the effect of phase noise and detecting distance on velocity error in CW mode in VCO design. The analysis shows that the effect of phase noise on velocity error can be reduced by shortening the detecting distance. There's little difference in short-range velocity measurement between the dual mode radar with MMIC VCO and the CW radar with low phase noise oscillator.

## 1. INTRODUCTION

In the recent years, the demand of high performance millimeter wave radar is increasing. The K-band radars capable of vehicle collision avoidance or traffic information collection have been widely used in the commercial market [1–5]. However, most commercial millimeter radar works in the single mode, which can not meet the needs in Intelligent Transportation Systems. Thus the dual-mode or multi-mode radar will play an important role [6–11], especially in accurate traffic information collection.

According to the Ambiguity Function of the radar waveform, FMCW radar has advantages in range measurement, the same as CW radar in velocity measurement [12–14]. The dual mode radar presented in this paper combines radar in two designs can make a

† M.-H. Yang and J. Xu are also with Graduate School of CAS, Beijing 100039, China

good performance in both range and velocity measurement, which is important in traffic information collection.

The marked difference between FMCW radar and CW radar is the oscillator. In FMCW radar the oscillator is VCO with the features of high linearity and wide modulation bandwidth. However, in CW radar the oscillator is DRO or PLL, which has low phase noise and high frequency stability [15–17]. Although the oscillators are different, the above two radar systems can be realized with the same RF front-end platform by using MMIC VCO as oscillator and choosing different modulation waveform. According to the above idea, a K-band dual mode radar is introduced in Section 2. As the phase noise of MMIC VCO is usually higher than DRO and PLL, the effect of phase noise and detecting distance on velocity error in CW mode is analyzed in Section 3, which proves that the dual-mode radar with MMIC VCO as oscillator can be used in short-range velocity measurement in CW mode. At last, the velocity measurement result and the comparison between the dual-mode radar and the CW radar with low phase noise PLL are given in Section 4.

## 2. MINIATURE K-BAND DUAL MODE RADAR

The dual mode radar is realized by choosing different modulation waveforms for VCO. The modulation waveform for VCO in FMCW mode is triangular, while in CW mode is constant voltage, which is shown in Figure 1. The modulation waveforms and IF signal processing circuits for different radar mode can be selected by analog switches. According to the above idea, the dual mode radar is designed. The block diagram of the radar front-end is shown in Figure 2. The photograph of the radar front-end is shown in Figure 3.

The radar is installed above the lane to collect the traffic

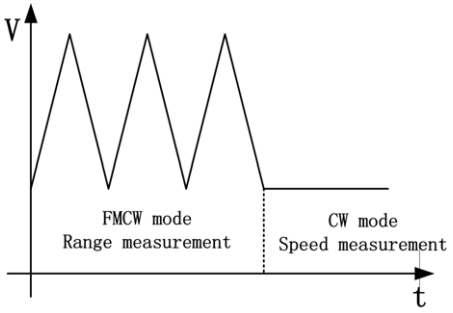


**Figure 1.** The modulation waveform.

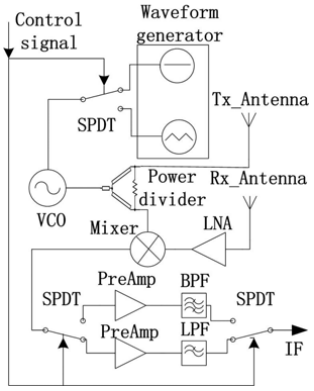


**Figure 2.** Block diagram of the radar front-end.

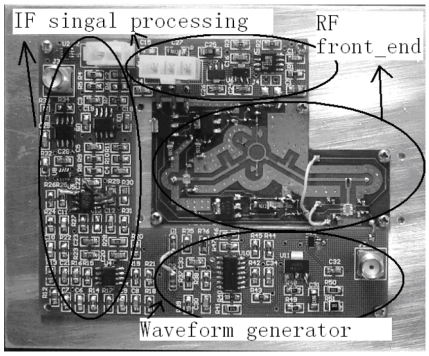


**Figure 3.** The photograph of the radar front-end.

information. According to the traffic situation of the road, the radar can automatically select corresponding radar mode. When the traffic situation is smooth, the radar utilizes the theory of measuring velocity to measure vehicle flow and vehicle velocity in CW mode. Besides, when vehicles are blocked or moving in very slow velocity, the radar will work in FMCW mode and utilize the theory of measuring distance to measure vehicle flow. The measured quantities of the dual mode radar are shown in Table 1.

**Table 1.** Measured quantities of the dual mode radar.

| Mode | Traffic situation | Traffic volume | Average speed | individual speed | Vehicle classification | Vehicle presence | Lane occupancy |
|---|---|---|---|---|---|---|---|
| CW | congested | ✓ | ✓ | ✓ | ✓ | ✓ | ✓ |
| FMCW | smooth | ✓ | ✓ | × | ✓ | ✓ | ✓ |

For low cost and compactness, MMIC technologies are used in VCO and LNA design. Wide modulation bandwidth, which is important for reducing ranging error in FMCW mode, can be easily reached in MMIC VCO design. However, the phase noise of MMIC VCO with wide modulation bandwidth is much higher than that of PLL or dielectric resonator usually used in CW radar. Thus the effect of phase noise on velocity error in CW mode should be analyzed in MMIC VCO design.

## 3. THE ANALYSIS OF VELOCITY ERROR IN CW MODE

In CW mode, the relational expression between the velocity error and the frequency stability of the oscillator is

$$\sigma_k^2 = \left(\frac{c}{2}\right)^2 \cdot 2 \cdot B_2(\gamma, \mu) \cdot \sigma_y^2(\tau) \tag{1}$$

where $B_2(\gamma, \mu)$ is Bias function for variances based on finite samples of a process with a power law spectral density, $\sigma_y^2(\tau)$ is Allan variance, $\gamma = \tau'/\tau$, $\tau'$ is time interval between the beginnings of two successive measurements of average frequency, $\tau$ is duration of average sampling period, and $\mu$ is exponent of noise model. As shown in Equation (1), $B_2(\gamma, \mu)$ and $\sigma_y^2(\tau)$ are the key to velocity error.

### 3.1. The Effect of Phase Noise on Velocity Error

Although $\sigma_y^2(\tau)$ can not be easily measured, it can be estimated from the phase noise. The phase noise of the oscillator is characterized by normalized spectral density of frequency fluctuations $S_y(f)$, which is in the form of the power-low noise process

$$S_y(f) = \sum_{\alpha=-2}^{2} h_\alpha f^\alpha, \quad 0 < f < f_h \quad S_y(f) = 0, \quad f_h < f \tag{2}$$

where $f_h$ is upper cutoff frequency, and $h_\alpha$ is constant of power-low noise. For a given type of oscillator two or more terms of the sum is dominant.

The calculation of $\sigma_y^2(\tau)$ can be derived from $S_y(f)$ [19].

$$\sigma_y^2(\tau) = 2\int_0^\infty S_y(f)\frac{\sin^4(\pi f\tau)}{(\pi f\tau)^2}df \tag{3}$$

When $2\pi f_h\tau \gg 1$, five common power-low noise processes, which are listed in Table 2 [19], is derived from Equation (3).

In Table 2, $h_\alpha$ stands for single-sideband phase noise $L(f)$, which can be estimated by Lesson's model or measured by spectrum analyzer.

The relational expression between $L(f)$ and $S_y(f)$ is

$$S_y(f) = \sum_{\alpha=-2}^{2} h_\alpha f^\alpha = 2\frac{f^2}{f_0^2}L(f) \tag{4}$$

During the five power-low phase noise, the white frequency noise ($\alpha = 0$), the broadband noise shaped by resonator $Q$ in oscillators, and the flicker frequency noise ($\alpha = -1$), the resonator noise and active component noise in oscillator, are both within the resonator bandwidth. In order to get wide modulation bandwidth, the resonator-loaded quality factor $Q$ of VCO can not be very high. Thus the two kinds of frequency noise are the main components of the phase noise. This gives rises to $L(f)$ plot consisting of three different regions, which is shown in Figure 4 [20].

As shown in Figure 4, $L(f)$ of VCO is usually characterized by three power-law function $K_{-3}f^{-3}$, $K_{-2}f^{-2}$ and $K_0f^0$. According to Equation (4), the relational expression between $h_{(n)}$ and $K_{n-2}$ is

$$h_{(n)} = \frac{2}{f_0^2} K_{(n-2)}, \quad n = -1, 0, 2 \tag{5}$$

where $K_{n-2}$ can be measured by spectrum analyzer. Thus according to Equation (5) and Table 2, $\sigma_y^2(\tau)$ can be calculated.

**Table 2.** $\sigma_y^2(\tau)$ for various power-low noise.

| Names of noise | $\alpha$ | $\sigma_y^2(\tau)$ |
|---|---|---|
| Random-walk frequency | $-2$ | $\frac{2\pi^2\tau h_{-2}}{3}$ |
| Flicker frequency | $-1$ | $2(\ln(2))h_{-1}$ |
| White frequency | 0 | $\frac{h_0}{2\tau}$ |
| Flicker phase | 1 | $\frac{(1.0385 + 3\ln(2\pi f_h\tau))h_1}{(2\pi)^2\tau^2}$ |
| White phase | 2 | $\frac{3f_h h_2}{(2\pi)^2\tau^2}$ |

According to the analysis of the preceding context, reducing the white frequency noise and flicker frequency noise in MMIC VCO design is very critical for decreasing the velocity error.

For the offsets beyond 10 KHz–1 MHz, the phase noise mainly depends on the high frequency noise properties of the device.

The HEMT technologies are superior to all other technologies. Consequently, 0.25 μm GaAs PHEMT technology is chosen in MMIC VCO design.

Furthermore, some conditions are satisfied in the practical MMIC VCO design in order to reduce the white frequency noise and flicker frequency noise. The first step is to put the transistor at the operating point where it provides the maximum added power. Second, one should dissipate the maximum of the power in the resonator, which is the main storage element of the circuit, to maximize its stored energy. Third, one must transfer this stored energy to the transistor controlling voltage port and output port where the Flicker frequency noise conversion into phase noise takes place by adjusting the phase difference between the resonator voltage, on one hand, and the transistor controlling voltage and output voltage on the other hand. According to the above design condition, the MMIC VCO has been designed and fabricated, the power spectrum of which is measured by Spectrum analyzer Anritsu MS2668C and is shown in Figure 5. The phase noise of the MMIC VCO is −77 dBc/Hz@100 KHz.

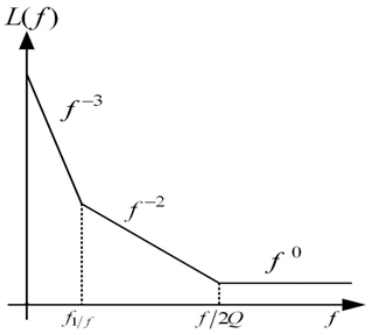


**Figure 4.** $L(f)$ in low $Q$ case.

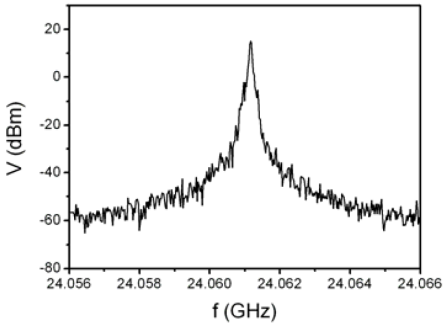


**Figure 5.** Phase noise performance of the VCO.

### 3.2. The Effect of Detecting Distance on Velocity Error

In addition to the phase noise, the detecting distance has quite an effect on velocity error. The detecting distance is related to $B_2(\gamma, \mu)$. When $2\pi f_h \tau \gg 1$ and $\gamma \ll 1$, $B_2(\gamma, \mu)$ is listed in Table 3 [18], where $\gamma$ is proportional to the distance between radar and target. According to Table 3, it's easily to get the fact that short detecting distance will lead to low velocity error.

**Table 3.** $B_2(\gamma, \mu)$ for various power-low noise.

| $\alpha$ | $B_2(\gamma, \mu)$ |
|---|---|
| $-1$ | $\frac{\ln 2}{4} \cdot \left[-2\gamma^2 \ln \gamma + (1+\gamma)^2 \ln(1+\gamma) + (1-\gamma)^2 \ln\lvert\gamma - 1\rvert\right]$ |
| 0 | $6\gamma$ |
| 2 | $2/3$ |

According to Table 2, Table 3 and Figure 4, the velocity error is expressed as:

$$\begin{aligned}\sigma_k^2 &= \frac{c^2}{2} \cdot \left\{ h_{-1} \cdot \frac{(\ln 2)^2}{2} \cdot \left[-2\gamma^2 \ln \gamma + (1+\gamma)^2 \ln(1+\gamma) \right.\right. \\ &\quad \left.\left. +(1-\gamma)^2 \ln|\gamma - 1|\right] + \frac{h_0}{\tau} \cdot 3\gamma + \frac{f_h h_2}{2\pi^2 \tau^2} \right\} \\ &= \frac{c^2}{2} \cdot 10^{P_{1/f}/10} \cdot \left\{ f_{1/f}^3 \cdot \frac{(\ln 2)^2}{2} \cdot \left[-2\gamma^2 \ln \gamma + (1+\gamma)^2 \ln(1+\gamma) \right.\right. \\ &\quad \left.\left. +(1-\gamma)^2 \ln|\gamma - 1|\right] + \frac{f_{1/f}^2}{\tau} \cdot 3\gamma + \frac{f_h \cdot f_{1/f}^2}{2\pi^2 \tau^2 \cdot f_{2Q}} \right\} \end{aligned} \quad (6)$$

where $P_{1/f}$ (dBc/Hz) is the phase noise in $f_{1/f}$.

According to Equation (6), short detecting distance and low phase noise, presented as low $1/f$ noise, both lead to reducing velocity error. However, VCO usually has a poorer phase noise than PLL and DRO. Thus short detecting distance is important for low velocity error.

Based on the above analysis, the velocity error is calculated as follow. From the spectrum shown in Figure 5, we can get $K_{-3} = 10^{7.3}$, $K_{-2} = 10^{1.2}$, $K_0 = 10^{-12.5}$ and $f_h = 100\,\text{MHz}$.

If the distance between radar and target is 100 m, $\tau'$ is $6.67 \times 10^{-7}$ s. As the dual mode radar is used in traffic information collection, the detecting velocity is usually below 180 KM/H. Thus the Doppler frequency is below 8 KHz. The sampling frequency is set to be 4 times the max Doppler frequency. Consequently, $\tau$ is $4.16 \times 10^{-5}$ s, and $\gamma$ is 0.016.

According to above calculation and analysis, the velocity error is:

$$\begin{aligned}\sigma_k &= \sqrt{\sigma_{k(-1)}^2 + \sigma_{k(0)}^2 + \sigma_{k(2)}^2} \\ &= \sqrt{2.1609 + 2.855 + 0.1446} = 2.27\,\mathrm{m/s} = 8.17\,\mathrm{KM/H} \end{aligned} \quad (7)$$

As shown in Equation (7), the flicker frequency noise and white frequency noise has a significant effect on velocity error when detecting distance is 100 m. The velocity error 8.17 KM/H is too high for traffic information collection.

However, when the detecting distance is 10 m, which is the typical distance for traffic information collection radar, the velocity error is:

$$\begin{aligned}\sigma_k &= \sqrt{\sigma_{k(-1)}^2 + \sigma_{k(0)}^2 + \sigma_{k(2)}^2} \\ &= \sqrt{0.0304 + 0.2855 + 0.1446} = 0.679\,\mathrm{m/s} = 2.44\,\mathrm{KM/H} \end{aligned} \quad (8)$$

As shown in Equation (8), the effect of flicker frequency noise and white frequency noise on velocity error will gradually weaken with the detecting distance decreased. On the contrary, the white phase noise will gradually dominate the velocity error in short-range velocity error. In addition, as $B_{2(1)}$ is a constant, the velocity error has a minimum 1.87 KM/H. In this situation, reducing the white phase noise is the only way to reduce velocity error. When detecting distance is 10 m, the velocity error 2.44 KM/H meets the needs of velocity measurement in traffic information collection.

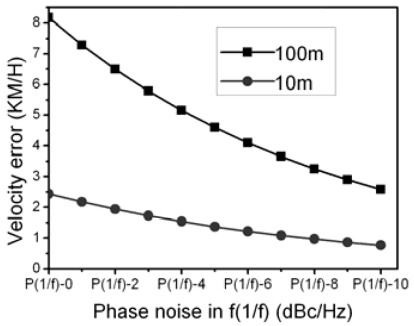


**Figure 6.** Phase noise-velocity error.

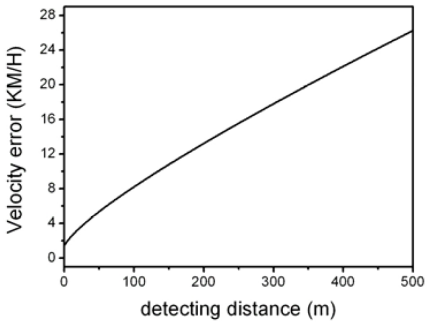


**Figure 7.** Distance-velocity error.

In different distances reducing the same phase noise has different effects on velocity error, which is proved by Equation (6). As shown in Figure 6, when the detecting distance is 100 m, reducing phase noise could significantly decrease velocity error. However, the effect

of reducing phase noise on decreasing velocity error is not distinctive when the detecting distance is 10 m. For the MMIC VCO used in the dual-mode radar, the plot of distance-velocity error is shown in Figure 7. According to Figure 6 and Figure 7, the velocity error will decrease with shortening the detecting distance. Although the phase noise of MMIC VCO is poor for long range velocity measurement, the dual mode radar is suitable for short range velocity measurement when working in CW mode.

## 4. THE VELOCITY MEASUREMENT EXPERIMENT

The dual mode radar with MMIC VCO mentioned in above paragraph is installed above the lane to measure the velocity of the car. The detecting distance is only 7 m. Figure 8 and Figure 9 are the waveform and frequency spectrum of the IF signal when the dual mode radar work in CW mode.

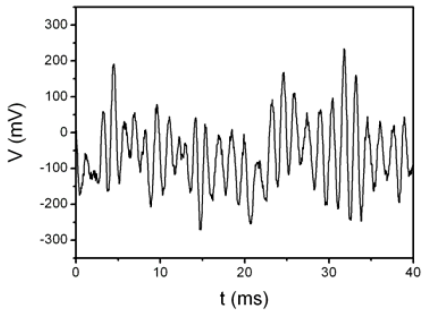


**Figure 8.** The waveform of the IF signal in CW mode.

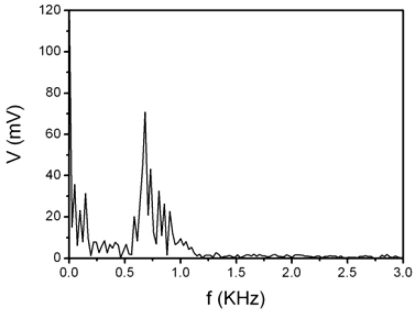


**Figure 9.** The spectrum of the IF signal in CW mode.

As shown in Figure 9, the max amplitude of frequency is 700 Hz. According to Doppler principle, the velocity of target is:

$$V = \frac{f_I \cdot C}{2f_0} = 15.75\,\text{KM/H} \tag{9}$$

The actual velocity of the car as target is 16 KM/H. The experiment result is in agreement with the theoretical value within the limit of experiment error.

In order to compare with other CW radar with low phase noise oscillator in velocity measurement, a CW radar with a K-band digital phase locked loop (PLL) frequency generator as oscillator is designed and fabricated. The PLL is a fourth-order negative phase feedback loop

which comprises reference crystal, commercial frequency synthesizer chip (HM533LP4, 24.128 GHz VCO), loop low pass filter and micro control unit (MCU). The PLL is shown in Figure 10. The phase noise of the PLL is −67 dBc/Hz@1 KHz, which is much lower than that of the MMIC VCO used in the dual-mode radar.

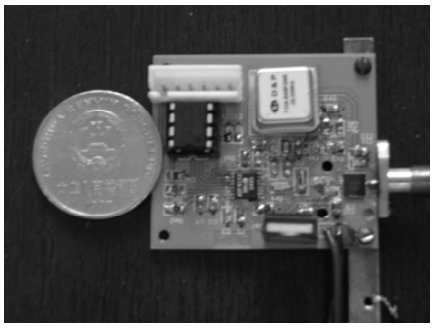

**Figure 10.** The 24 GHz PLL.

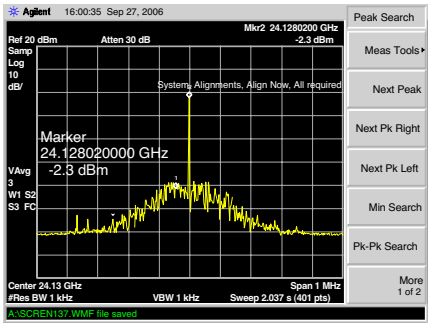


**Figure 11.** Phase noise performance of the PLL.

The phase noise of the oscillator is reduced by the feedback only within the bandwidth of the loop. When the offset is larger than the loop bandwidth, total PLL phase noise is nearly the same as the free running VCO. As shown in Figure 11, only the $f^{-3}$ (Flicker frequency) noise appears to be reduced. According to the discussion in Section 3, the effect of Flicker frequency noise on velocity error will decrease when the detecting distance is shortened.

The two radar with low phase noise PLL and MMIC VCO separately have been used to measure the velocity of the same car. The result for comparison is shown in Table 4.

**Table 4.** Comparison between two radar.

| | 10 m | 20 m | 30 m |
|---|---|---|---|
| The radar with PLL | 20.6 KM/H | 25.5 KM/H | 35.8 KM/H |
| The dual mode radar | 21.3 KM/H | 24.9 KM/H | 36.9 KM/H |

As shown in Table 4, there's little difference in short-range velocity measurement between the CW radar with low phase noise PLL and the dual mode radar with MMIC VCO. Therefore the dual mode radar can be used in short-range velocity measurement and traffic information collection.

## 5. CONCLUSION

The K-band dual mode radar referred in this paper can work in both FMCW mode and CW mode. According to the analysis of the effect of phase noise and detecting distance on velocity error, the dual mode radar meets the needs of short-range velocity measurement.

## REFERENCES

1. Russell, M. E. and C. Arthur, "Millimeter-wave radar sensor for automotive Intelligent Cruise Control (ICC)," *IEEE Transactions on Microwave Theory and Techniques*, Vol. 45, No. 12, 2444–2453, 1997.
2. Singh, A. K., P. Kumar, T. Chakravarty, G. Singh, and S. Bhooshan, "A novel digital beamformer with low angle resolution for vehicle tracking radar," *Progress In Electromagnetics Research*, PIER 66, 229–237, 2006.
3. Xue, W. and X. W. Sun, "Target detection of vehicle volume detecting radar based on Wigner-Hough transform," *Journal of Electromagnetic Waves and Applications*, Vol. 21, 1513–1523, 2007.
4. Cui, B., J. Zhang, and X. W. Sun, "Single layer microstrip antenna arrays applied in millimeter-wave radar front-end," *Journal of Electromagnetic Waves and Applications*, Vol. 22, 3–15, 2008.
5. Shi, X., F. Wei, Q. Huang, L. Wang, and X.-W. Shi, "Novel binary search algorithm of backtracking for RFID tag anti-collision," *Progress In Electromagnetics Research B*, Vol. 9, 97–104, 2008.
6. Roberton, M. and E. R. Brown, "Integrated radar and communications based on chirped spread-specturm," *IEEE MTT-S*, 2003.
7. Conn, M., F. Koenig, G. Goldman, and E. Adler, "Waveform generation and signal processing for a multifunction radar system," *IEEE Radar Conference*, 2004.
8. Haridim, M., H. Matzner, Y. Ben-Ezra, and J. Gavan, "Cooperative targets detection and tracking range maximization using multimode ladar/radar and transponders," *Journal of Electromagnetic Waves and Applications*, Vol. 18, 1105–1117, 2004.
9. Li, Z. and K. Wu, "24 GHz radar front-end for FMCW and spread spectrum radar applications," *Radio and Wireless Symposium, 2006 IEEE*, 351–354, 2006.
10. Ku, H. S. and T. Yusaf, "Processing of composites using

variable and fixed frequency microwave facilities," *Progress In Electromagnetics Research B*, Vol. 5, 185–205, 2008.

11. Ren, W., "Compact dual-band slot antenna for 2.4/5 GHz WLAN applications," *Progress In Electromagnetics Research B*, Vol. 8, 319–327, 2008.
12. Stove, A. G., "Linear FMCW radar techniques," *Radar and Signal Processing, IEE Proceedings F*, Vol. 139, No. 5, 343–350, 1992.
13. Wang, C. J., B. Y. Wen, Z. G. Ma, W. D. Yan, and X. J. Huang, "Measurement of river surface currents with UHF FMCW radar systems," *Journal of Electromagnetic Waves and Applications*, Vol. 21, 375–386, 2007.
14. Alivizatos, E. G., M. N. Petsios, and N. K. Uzunoglu, "Towards a range-doppler UHF multistatic radar for the detection of non-cooperative targets with low RCS," *Journal of Electromagnetic Waves and Applications*, Vol. 19, 2015–2031, 2005.
15. Saliminejad, R. and M. R. GhafouriFard, "A novel and accurate method for designing dielectric resonator filter," *Progress In Electromagnetics Research B*, Vol. 8, 2935–306, 2008.
16. Chang, H.-W., "Field analysis of dielectric waveguide devices based on coupled transverse-mode integral equation — Mathematical and numerical formulations," *Progress In Electromagnetics Research*, PIER 78, 329–347, 2008.
17. De, A. and G. V. Attimarad, "Numerical analysis of two dimensional tapered dielectric waveguide," *Progress In Electromagnetics Research*, PIER 44, 131–142, 2004.
18. Barnes, J. A., "Characterization of frequency stability," *IEEE Trans. IM*, Vol. 20, No. 2, 105, 1971.
19. Rutman, J. and F. L. Walls, "Characterization of frequency stability in precision frequency sources," *Linear FMCW Radar Techniques, Proceedings of the IEEE*, Vol. 79, No. 7, 952–960, 1991.
20. Drucker, E., "Model PLL dynamics and phase-noise performance," *Microwaves & RF*, Vol. 2000, No. 2, 73–82, 2002.